3 Biotech (2023) 13:299
https://doi.org/10.1007/s13205-023-03686-w

ORIGINAL ARTICLE

Production of anti-inflammatory films based on cashew gum polysaccharide and polyvinyl alcohol for wound dressing applications

Cassio N. S. Silva[1] · Maurício V. Cruz[1,2] · Kátia F. Fernandes[1] · Karla A. Batista[1,3]

Received: 7 February 2023 / Accepted: 25 June 2023 / Published online: 11 August 2023

Abstract

In the present study, we aimed to produce CGP/PVA films containing entrapped anti-inflammatory drugs for wound dressing applications. Using a 3^{3-1} fractional factorial design, the effect of each component was evaluated on the physicochemical and morphological properties of the produced materials. The best formulation for entrapment of diclofenac sodium and ketoprofen was also determined. The produced films presented high swelling capacity, with some formulations showing o porous structure. CGP/PVA films showed a maximum retention of 75.6% for diclofenac sodium and 32.2% for ketoprofen, and both drugs were released in a controlled manner for up to 7 h. The drug release kinetic was studied, and the data were fitted using a Korsmeyer–Peppas model, which suggested that the release mechanism is controlled by diffusion. These results indicate that CGP/PVA-based matrices have great potential to be used as drug–delivery systems for wound dressing applications, contributing to prolonging the drug's action time and then improving their anti-inflammatory efficacy.

Keywords Natural polymers · Drug delivery · Controlled release · Wound care · Wound healing

Introduction

Chronic wounds affect patients' quality of life and have considerable economic and social impacts. In general, chronic wounds are a result of a failure in the regulation of the natural healing process, with a prolonged or excessive inflammatory phase, persistent infection and delayed wound contraction being observed (Kaolaor et al. 2019; Katiyar et al. 2022). Chronic wound healing is a complex process that might last over 12 weeks (Shitole et al. 2019). In this case, appropriate wound care is crucial to improving the healing process and protecting the wound from infections and contamination. Wound dressings are critical for wound care, providing a physical barrier that protects the open wound from further trauma or infection. Along with protection and isolation, wound dressings can also provide a controlled release of drugs to alleviate pain and accelerate healing (Sharma et al. 2020; Nissi et al. 2023).

Polymeric wound dressing materials based on natural polymers have been intensively studied in recent years, helping combat bacterial infection, stimulating wound healing, acting as powerful absorbents of the excess fluids released in the wound, and also providing a bio-mimic microenvironment that fastens the wound repair process (Sharma et al. 2020; Abdel-Mageed et al. 2022; Chandika et al. 2021; Feng et al. 2021). Among the different natural polymers currently studied in wound dressing applications, cashew gum polysaccharides (CGP) have gained attention due to their excellent biocompatibility, biodegradability, inertness and film-forming ability (Moreira et al. 2015; Silva et al. 2016; Lima et al. 2018; Cruz et al. 2019a).

However, bioactive wound dressing films composed only of CGP are limited by their high water solubility, poor mechanical strength and low stability (Moreira et al. 2020). To overcome these limitations, in the last decade, we have

Cassio N. S. Silva, Maurício V. Cruz have contributed equally to this work.

✉ Karla A. Batista
karla.batista@ifg.edu

[1] Laboratório de Química de Polímeros, Departamento de Bioquímica e Biologia Molecular, Instituto de Ciências Biológicas 2, Campus Samambaia, Universidade Federal de Goiás, Goiânia, GO 74690-900, Brazil

[2] Departamento de Áreas Acadêmicas II, Instituto Federal de Educação, Ciência e Tecnologia de Goiás, Campus Goiânia, Goiânia, GO 74055-120, Brazil

[3] Departamento de Áreas Acadêmicas, Instituto Federal de Educação, Ciência e Tecnologia de Goiás, Campus Goiânia Oeste, Goiânia, GO 74395-160, Brazil

studied the effect of blending CGP with polyvinyl alcohol (PVA), a widely explored synthetic polymer for wound dressing and wound management, which presents desirable features such as biocompatibility, biodegradability, bioadhesiveness, non-toxicity, film-forming ability and ease of processing (Kaolaor et al. 2019; Shitole et al. 2019). Different formulations of CGP/PVA films were studied as matrices for several purposes, especially in the preparation of bioactive and biodegradable materials to be used in biomedicine (Moreira et al. 2015; Silva et al. 2016; Cruz et al. 2019a; Chagas et al. 2022).

The combination of CGP and PVA enabled the production of biocompatible and biodegradable films with excellent mechanical properties and a high capacity to encapsulate and release molecules in a controlled manner (Moreira et al. 2015; Silva et al. 2016; Cruz et al. 2019a). The bioactive potential associated with the good properties of stability of the matrix and the possibility of storing CGP/PVA films dried or in solution over time without losing their mechanical, physicochemical, and biological properties are advanced characteristics that enable the purposing CGP/PVA as an efficient bio-based material to be used as a bifunctional agent helping the healing process while protects the wound from injuries and contaminations (Moreira et al. 2015; Silva et al. 2016; Chagas et al. 2022).

We have recently demonstrated that CGP/PVA films have shown a slow in vivo biodegradability and a biocompatibility pattern classified as non-irritating material (Chagas et al. 2022). Altogether, these chemical and biological properties of CGP/PVA films make them promising materials to be explored as matrices for developing membranes for skin wound healing.

The ability of CGP/PVA films to efficiently entrap bioactive molecules might be an essential characteristic of developing membranes acting as drug delivery systems. Considering that pharmacological treatments are often recommended to improve healing and suppress the pain associated with the wound healing process, the design of multifunctional dressings containing anti-inflammatory/analgesic molecules could enhance the effectiveness of wound management. In this scenario, it would be interesting the development of dressings containing medicine like non-steroidal anti-inflammatory drugs (NSAIDs), which present important effects in alleviating pain and inflammation (Shehata et al. 2020), by has some limitations regarding blood bioavailability and undesired side effects when administered orally (Khan et al. 2018; Al-Lawati et al. 2019).

Based on the disadvantages associated with oral therapy of NSAIDs, wound dressings acting as transdermal drug delivery systems could be an efficient alternative to improve patient compliance, enhance drug efficacy, avoid adverse side effects, and accelerate the wound healing process. Therefore, in the context of designing multifunctional wound dressings, this study aimed to produce polymer-based dressings based on CGP and PVA functionalized with two different NSAIDs, ketoprofen and diclofenac sodium. The CGP/PVA films were prepared using a 3^{3-1} fractional factorial design and characterized regarding their morphological and swelling properties. Furthermore, the entrapment efficiencies of ketoprofen and diclofenac sodium were evaluated, and the drug release profile was investigated.

Materials and methods

Chemical and reagents

Ethanol (95%) was purchased from Dinâmica Química Contemporânea Ltda. (São Paulo, SP, Brazil). Polyvinyl alcohol (product number 363138), Mannitol (98% purity), diclofenac sodium salt (98% purity) and ketoprofen (98% purity) were purchased from Sigma-Aldrich Chemical Co. (St. Louis, MO, USA). All other chemicals used were of analytical grade, obtained from accredited companies and were used as received.

Isolation of CGP

Samples of cashew gum were obtained from *Anacardium occidentale* trees in Aquirás, Ceará, Brazil. Polysaccharide isolation was then performed according to the methodology described by Silva et al. (2016). Briefly, the nodules were milled, immersed in distilled water in a proportion of 1:5 (*w*/*v*) and kept at room temperature (25 °C), for 24 h, under stirring. The suspension was filtered to remove bark fragments and then precipitated with cold ethanol at a 1:3 concentration (v/v). The precipitated polysaccharide (CGP) was separated by centrifugation, washed with cold ethanol and dried at room temperature. The white pellets were milled and stored at room temperature in airtight vials.

Production of the CGP/PVA films

Experimental design

The CGP/PVA films were prepared using a solvent-casting technique from their film-forming dispersions. The effects of polymer concentration and oxidizing agent content on the film's properties and drug entrapment efficiency were evaluated using a 3^{3-1} fractional factorial design. The experiments were performed using the following setting values (independent factors):

- CGP concentration: 1% (*w*/*v*) (low level); 2% (*w*/*v*) (central point) and 3% (*w*/*v*) (high level);

- PVA concentration: 3% (*w*/*v*) (low level); 4.5% (*w*/*v*) (central point) and 6% (*w*/*v*) (high level); and
- $NaIO_4$ concentration: 0.5 mol L^{-1} (low level); 0.75 mol L^{-1} (*w*/*v*) (central point) and 1.0 mol L^{-1} (*w*/*v*) (high level).

The arrangement of variables and levels used in the film-forming dispersions are shown in Table 1.

Results from the 3^{3-1} fractional factorial design were analyzed using the software Statistica (Statistica 10.0 StatSoft Inc., Tulsa, OK, USA). The adjustment of the experimental data for the independent variables in the RSM was represented by the second-order polynomial equation:

$$y = \beta_0 + \sum_{i=1}^{k} \beta_i x_i + \sum_{i=1}^{k} \beta_i x_i^2 + \sum_{i<j}^{k} \beta_{ij} x_i x_j, \quad (1)$$

where y is the measured variable; β_0, β_i, and β_j are regression coefficients, and x_i /x_j are the independent variables. The model was simplified by dropping terms that were not statistically significant ($p > 0.01$) by ANOVA.

Film production

The film-forming dispersions were prepared by mixing 100 mL PVA solution with 100 mL of CGP solution, 10 mL of sodium metaperiodate solution ($NaIO_4$) as an oxidizing agent, 20 mL of 1.0 mol L^{-1} phosphoric acid solution (H_3PO_4) as the catalyst, and 30 mg of mannitol as a plasticizer. This film-forming dispersion was cast onto acrylic molds and the solvent evaporation was left to occur at room temperature (25 °C ± 2 °C). The dried films were peeled from the casting molds, washed with distilled water to completely remove unreacted materials, dried at room temperature and stored in plastic vials.

Table 1 Independent variables and levels established by the 3^{3-1} fractional factorial design for producing the CGP/PVA films

Formulation	CGP (%) X_1	PVA (%) X_2	$NaIO_4$ (mol L^{-1}) X_3
F1	1.0 (–)	3.0 (–)	0.5 (–)
F2	2.0 (0)	3.0 (–)	1.0 (+)
F3	3.0 (+)	3.0 (–)	0.75 (0)
F4	1.0 (–)	4.5 (0)	1.0 (+)
F5	2.0 (0)	4.5 (0)	0.75 (0)
F6	3.0 (+)	4.5 (0)	0.5 (–)
F7	1.0 (–)	6.0 (+)	0.75 (0)
F8	2.0 (0)	6.0 (+)	0.5 (–)
F9	3.0 (+)	6.0 (+)	1.0 (+)

Characterization of the CGP/PVA films

Swelling behavior

The swelling behavior of the CGP/PVA films was determined according to Sabbagh et al. (2018), with minor modifications. For the test, strips of 1 cm^2 were weighted, immersed in 5 mL of distilled water and allowed to soak for 60 min at room temperature. The swollen films were taken out of the solution at regular intervals, weighed and replaced in the same solution to ensure a state of equilibrium. The swelling capacity of CGP/PVA films was calculated using the following equation:

$$\text{Swelling capacity}(\%) = \left(\left[W_s - W_d\right]/W_d\right) \times 100, \quad (2)$$

where W_s represents the weight of the swollen CGP/PVA film at time *t,* and W_d represents the dried weight of the sample.

Morphological analysis

Aiming to investigate the effect of swelling on the microstructure of CGP/PVA films, the swollen films were frozen, lyophilized and then examined through scanning electron microscopy, (JEOL JSM 6610 microscope) using a secondary electron detector with 15 kV of acceleration. The pore size was determined using the Fiji software (Schindelin et al. 2012). The average pore size was determined after at least 20 individual measures by an open field, with three different areas evaluated during SEM analysis. Experiments and analyses involving high-resolution microscopy were performed in the Multi-user High Resolution Microscopy Lab/Laboratório Multiusuário de Microscopia de Alta Resolução (LabMic) at the Universidade Federal de Goiás, GO, Brazil.

Entrapment of diclofenac sodium and ketoprofen onto CGP/PVA films

The produced CGP/PVA films were tested for entrapment of non-steroidal anti-inflammatory drugs (NSAIDs). This study used diclofenac sodium and ketoprofen as model drugs, at 10 mg mL^{-1}. Samples of CGP/PVA films (1 cm^2) were immersed in 1 mL of drug solution for 24 h at room temperature. The amount of unentrapped drug was quantified spectrophotometrically in the remaining solution ($\lambda_{diclofenac} = 280$ nm; $\lambda_{ketoprofen} = 255$ nm). The entrapment efficiency (%EE) was calculated, as shown in the following equation:

$$\%\,EE = \left(\left[\text{total drug} - \text{free drug}\right]/\text{total drug}\right) \times 100 \quad (3)$$

In vitro drug release

In vitro drug release was performed according to the methodology described by Liu et al. (2016). The CGP/PVA films containing ketoprofen (CGP/PVA–KET) or diclofenac sodium (CGP/PVA–DIC) were immersed in sodium phosphate buffer solution (0.1 mol L^{-1}, pH 7.4) and incubated at 37 °C. Aliquots of 50 µL of the solution were withdrawn periodically, and the initial volume of the release medium was maintained by adding an equivalent amount of fresh phosphate buffer solution after each sampling. For quantification, 50 µL of the sample was diluted to 1 mL with phosphate buffer (1:20 dilution v/v) and the amount of drug present in the sample was determined using a UV–Vis spectrophotometer ($\lambda_{diclofenac} = 280$ nm; $\lambda_{ketoprofen} = 255$ nm).

Drug release kinetics

To analyze the mechanism of drug release, several models were applied to adjust experimental data using KinetDS 3.0 software (Mendyk and Jachowicz 2007). The zero-order model is expressed as the cumulative amount of drug released *vs* time, being determined by the following equation:

$$C = k_0 t, \tag{4}$$

where k_0 is the zero-order rate constant expressed in units of concentration/time and t is the time in minutes. A concentration vs. time graph would yield a straight line with a slope equal to k_0 and intercept the origin of the axes.

The first order model is defined as the logarithm of the cumulative percentage of drug remaining as function of time. This model can be expressed by the following equation:

$$\log C = \log C_0 - k \times (t/2.303), \tag{5}$$

where C_0 is the initial drug concentration, k is the first order constant and t is the time in minutes.

Higuchi's model can be defined as the cumulative percentage of drug released *vs* the square root of time, according to the following equation:

$$Q_t = k \times t^{1/2}, \tag{6}$$

where Q_t is the amount of drug released in time t, k is the kinetic constant and t is the time in minutes.

The Korsmeyer–Peppas model can be defined as a log cumulative percentage of drug released *vs* log time and the release exponent n and k value were calculated using the following equation:

$$M_t/M_\infty = k \times t^n, \tag{7}$$

where M_t is the amount of the released drug at time t, M_∞ is the total amount of drug released after an infinite time, k is the diffusional characteristic of the drug/polymer system constant and n is a diffusional exponent used to indicate the drug release mechanism (Ritger and Peppas 1987). Considering polymeric materials, it has been reported that values of $n \leq 0.45$ describe a Fickian diffusion (case I transport) release mechanism. If $0.45 < n < 0.89$ the releasing mechanism corresponds to a non-Fickian transport. When $n = 0.89$ the drug release mechanism occurs through polymer swelling (case II transport) and if $n > 0.89$ the erosion of polymer dictates the drug release (Kashani et al. 2021).

Statistical analysis

All analyses were performed at least in triplicate. Results from the 3^{3-1} fractional factorial design were analyzed by regression analysis coupled to response surface methodology (RSM), using the software Statistica 10.0 (Statsoft Inc., Tulsa, USA). The model was simplified by dropping terms that were not statistically significant ($p = 0.05$) by ANOVA.

Results and discussion

Model establishment

It is well-known that the type and amount of each component used for developing films and membranes for wound healing applications will dictate the chemical, structural, and functional properties of the produced biomaterial. In this study, the effect of polymers and oxidizing agent concentrations on the swelling behavior and efficiency of drug entrapment were investigated through a 3^{3-1} fractional factorial design, and the significance of the model was evaluated by one-way and two-way analysis of variance (ANOVA).

The quality of fit of the mathematical model to the experimental results was determined using the coefficient of determination values (Table 2), and a second-order polynomial model was adopted as an appropriate mathematical function. This model has chosen since it presented the highest values of r^2 and adj-r^2 for all responses compared to the other models (Table 2). The predicted r^2 value indicates how well the model could predict future data. However, a large value of r^2 only sometimes implies that the regression mode is suitable since it assumes that all the independent variables considered affect the result of the model, increasing with each variable addition, regardless of whether it is statistically significant. In this sense, the model accuracy is better explained by analyzing the adjusted-r^2 value, which considers only those independent variables that affect the model's performance. As can be observed in Table 2, all the modeled variables presented r^2 and adj-r^2 values very close,

Table 2 Model adequacy by ANOVA for the swelling and entrapment properties of the CGP/PVA films

Model	Swelling behavior	Dependent variables	
		Entrapment efficiency for diclofenac	Entrapment efficiency for ketoprofen
No interaction	$r^2 = 0.824$ adj-$r^2 = 0.771$	$r^2 = 0.991$ adj-$r^2 = 0.989$	$r^2 = 0.759$ adj-$r^2 = 0.687$
Two-way interaction (linear x linear)	$r^2 = 0.849$ adj-$r^2 = 0.794$	$r^2 = 0.992$ adj-$r^2 = 0.989$	$r^2 = 0.773$ adj-$r^2 = 0.689$
Two-way interaction (linear x quadratic)	**$r^2 = 0.962$ adj-$r^2 = 0.945$**	**$r^2 = 0.999$ adj-$r^2 = 0.999$**	**$r^2 = 0.999$ adj-$r^2 = 0.999$**

Bold values indicate $p = 0.05$

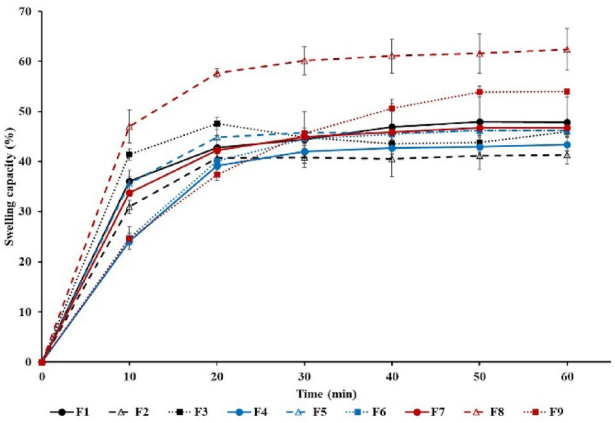

Fig. 1 Swelling profile of the CGP/PVA films produced according to the 3^{3-1} fractional factorial design. Results were presented as percentages of absorbed water into each film, and the vertical bars correspond to the standard deviation of the data

indicating that insignificant terms have not been included in the model. Furthermore, the r^2 and adj-r^2 values conclude that the applied statistical model effectively predicts the response.

After the model establishment, it was necessary to evaluate the significance of the effect estimates for each independent variable. It should be noted that the linear and quadratic terms for the oxidizing agent concentration were the factors that did not affect the swelling behavior of the CGP/PVA film. In addition, the entrapment efficiency, irrespective of the NSAID tested, was influenced by all independent variables.

Characterization of the CGP/PVA films

Swelling behavior

The swelling ability is a fundamental property that could influence drug release rates by controlling the diffusion rate of a drug into the polymer matrix and its dissolution and diffusion throughout the three-dimensional network of the swollen matrix (Piacentini et al. 2020). Moreover, the extent and rate of polymer swelling dictate the adsorption of exudates in wound healing products (Shitole et al. 2019; Abdel-Mageed et al. 2022). In this study, the swelling capacity of CGP/PVA films with different amounts of polymers and oxidizing agent was studied and the results are shown in Fig. 1. As can be observed, the equilibrium of swelling was reached after 20 min for all CGP/PVA films except for the formulation containing the higher concentrations of polymers and oxidizing agent (F9). For this formulation, stabilization of the swelling only occurred after 50 min. In addition, the swelling capacity ranged from 41.3 to 62.4% for the CGP/PVA films, with the formulation F8 (62.4%) and F9 (53.9%) showing the highest swelling values. The possibility of controlling the swelling behavior of CGP/PVA films by changing their component composition makes them very attractive for biomedical applications.

To evaluate the effect of the film constituents on the swelling behavior of the produced materials, a multivariate analysis was carried out using the swelling values after 60 min of incubation (Table 4). According to the significance degree of the terms extracted from the ANOVA results (Table 3), the data from swelling capacity were converted into a second-order polynomial equation describing the correlation between the response and the variables. The mathematical model is represented in the following equation:

$$\text{swelling capacity}(\%) = 167.94 - 87.02X_1 + 20.36X_1^2 - 35.09X_2 + 1.97X_2^2 + 22.52X_1X_2 - 5.27X_1^2X_2 \quad (r^2 = 0.96) \tag{8}$$

where X_1 denotes de concentration of CGP (%, *w*/*v*) and X_2 denotes de concentration of PVA (% *w*/*v*). The value of adj-r^2 (Table 2) indicates that 95.0% of the experimental data agreed with the predicted values, assuring that the experimental model can successfully explain this response.

Results from multivariate analysis also revealed that the most pronounced positive effect on the swelling capacity was obtained for the linear term of PVA concentration (Table 3). In addition, the linear and quadratic terms of CGP concentration and the interaction factors of CGP and PVA also positively affected the response. This result is expected considering the hydrophilic nature of these polymers since increasing the concentration of polymers will increase the number of polar groups in the polymer network available to interact with water. The branched structure of CGP (Fig. 2) significantly contributes to the polymeric matrix's relaxation ability. For this reason, the higher the amount of CGP, the

Table 3 Effect estimates coefficients for swelling and drug entrapment efficiency of the CGP/PVA films

Factor	Swelling		Entrapment efficiency for diclofenac		Entrapment efficiency for ketoprofen	
	Coefficient	*p* value*	Coefficient	*p* value	Coefficient	*p* value
Mean/Intercept	48.21	< 0.001	31.85	< 0.001	18.82	< 0.001
(X_1) CGP (L**)	1.88	< 0.001	– 11.65	< 0.001	20.00	< 0.001
CGP (Q***)	3.34	< 0.001	– 5.97	< 0.001	8.47	< 0.001
(X_2) PVA (L)	9.44	< 0.001	– 26.18	< 0.001	9.47	< 0.001
PVAL (Q)	– 4.45	< 0.001	– 8.12	< 0.001	7.56	< 0.001
(X_3) $NaIO_4$ (L)	**– 1.66**	**1.02**	30.44	< 0.001	15.30	< 0.001
$NaIO_4$ (Q)	**– 1.83**	**0.89**	– 33.68	< 0.001	2.68	< 0.001
X_1 by X_2	4.36	< 0.001	3.16	< 0.001	5.93	< 0.001
X_1^2 by X_2	7.89	< 0.001	– 8.24	< 0.001	21.10	< 0.001

*The values given in bold are not statistically significant

**Linear component (L)

***Quadratic component (Q)

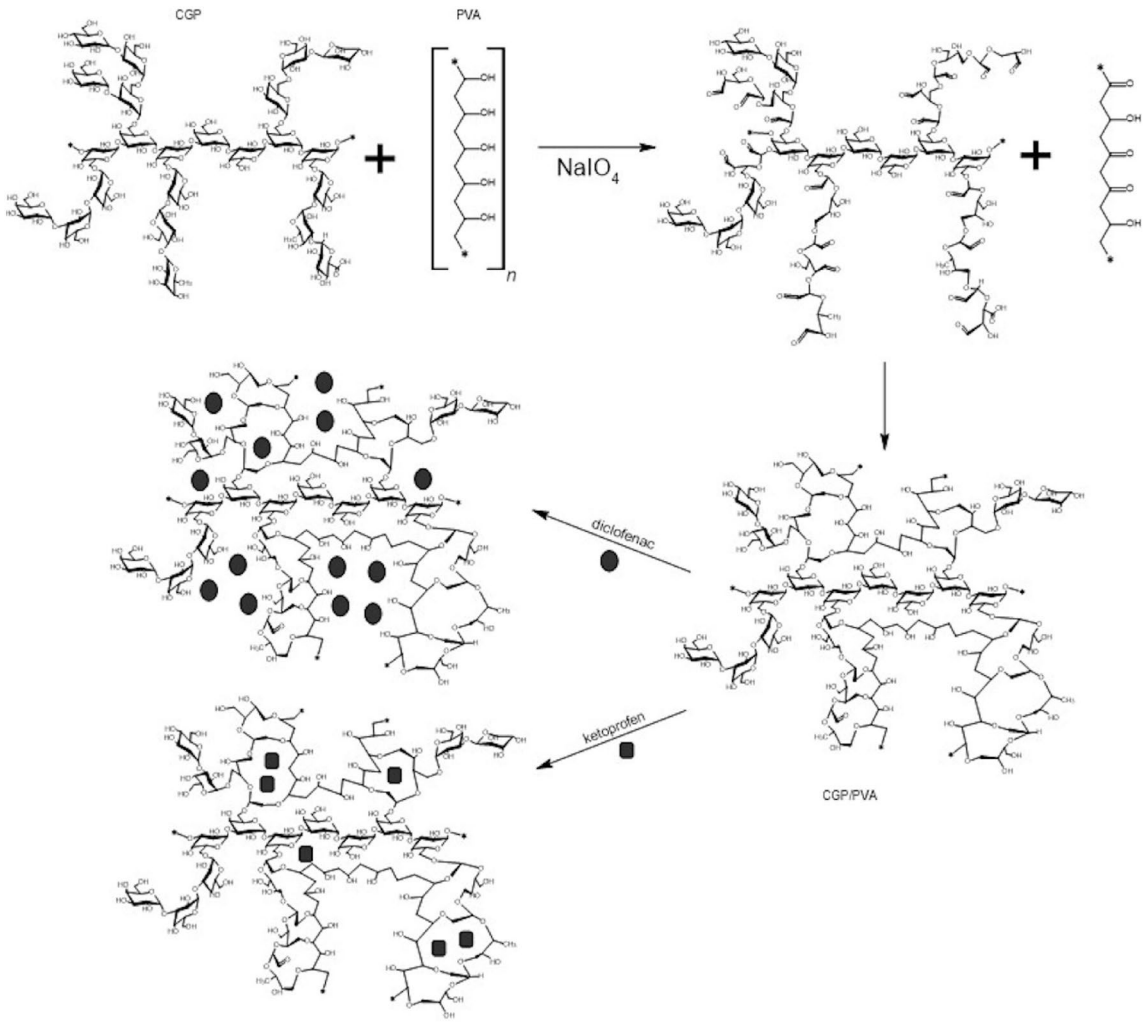

Fig. 2 Scheme representing the chemical interactions possibly occurring between the components of the CGP/PVA films during production and entrapment of diclofenac sodium and ketoprofen. *CGP* cashew gum polysaccharide, *PVA* polyvinyl alcohol, *$NaIO_4$* sodium metaperiodate, the oxidizing agent

Table 4 Results for the swelling capacity of the CGP/PVA films produced as established by the 3^{3-1} fractional factorial design

Formulation	CGP (%) X_1	PVA (%) X_2	$NaIO_4$ (mol L^{-1}) X_3	Swelling capacity (%)[a]
F1	1.0 (–)	3.0 (–)	0.5 (–)	47.8 ± 5.65
F2	2.0 (0)	3.0 (–)	1.0 (+)	41.3 ± 1.82
F3	3.0 (+)	3.0 (–)	0.75 (0)	45.9 ± 1.01
F4	1.0 (–)	4.5 (0)	1.0 (+)	43.4 ± 1.36
F5	2.0 (0)	4.5 (0)	0.75 (0)	46.2 ± 0.14
F6	3.0 (+)	4.5 (0)	0.5 (–)	46.2 ± 1.45
F7	1.0 (–)	6.0 (+)	0.75 (0)	46.7 ± 1.65
F8	2.0 (0)	6.0 (+)	0.5 (–)	62.4 ± 4.09
F9	3.0 (+)	6.0 (+)	1.0 (+)	53.9 ± 1.13

[a]The values are presented as means and standard deviations ($n = 6$)

higher the swelling capacity of the produced CGP/PVA films (Table 4). This increased fluid absorption capacity observed in the CGP/PVA film formulations constitutes an advantage for wound healing applications since they can provide controlled moisture in the injured microenvironment, avoiding infection and maceration in the wound bed (Enache et al. 2022; Paranhos et al. 2022).

On the other hand, while the quadratic term of PVA concentration negatively affected the swelling capacity, the content of $NaIO_4$ did not interfere with this response (Table 3). A large increase in the concentration of PVA may favor the occurrence of interactions between the liner chains of PVA (Fig. 2), which can result in a more cohesive matrix with a lower ability to relax in the presence of water.

The total of interactions between the CGP/PVA films and the solvent molecules is proportional to the number of available polar groups as well as the relaxation capacity of the polymer network (Fig. 2). In this sense, increasing the concentration of CGP and PVA in the formulations will increase the number of hydrophilic groups in the structure of the films, which will favor water molecules entering the three-dimensional network of the CGP/PVA films (Fig. 3). Furthermore, the presence of negatively charged centers along the chains of CGP might favor the relaxation of the film matrix as a result of a reorganization of the polymer chain entanglements due to the charge repulsion, which improves the swelling capacity of the CGP/PVA films (Fig. 2).

The high swelling power demonstrated by the CGP/PVA films contributes to: (1) increasing the adhesion of the film to the injured skin when it contacts the moist wound surface; (2) adsorbing the excess of wound exudates; (3) dictating the release of the therapeutic molecules entrapped in the matrix; and (4) the maintenance of a moist microenvironment on the wound surface. Considering that the commercially available medicated plaster could hinder the healing process because of some drawbacks related to their adhesion

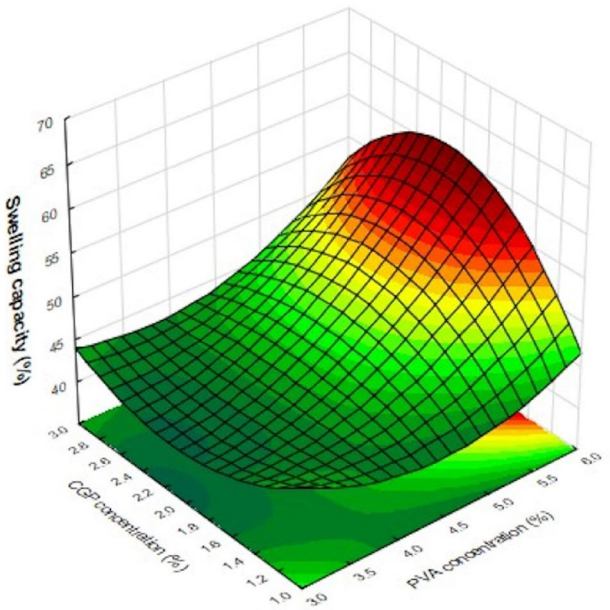

Fig. 3 Response surface plot obtained in the 3^{3-1} fractional factorial design for the swelling capacity of the CGP/PVA films as a function of the variables that significantly affected the response ($p < 0.05$). *CGP* cashew gum polysaccharide, *PVA* polyvinyl alcohol

properties and inhibition of the hydration of the wounds (Gudin and Nalamachu 2020; Enache et al. 2022), the swelling properties of CGP/PVA films together with the previously reported features of adhesion (Moreira et al. 2015) constitute and advance in the production of polymer-based plasters. Together with these properties, CGP/PVA films also provide physical protection that prevents the wound from further injuries, which contributes to accelerating the healing process.

Microstructural morphology of the swollen CGP/PVA films

SEM was used to verify if changes in the film formulations would influence their microstructure after swelling. SEM is a technique widely used to evaluate the microstructure of materials, allowing a better understanding of the properties and potentialities of a product. Before swelling, the CGP/PVA films showed a general uniform and smooth structure, without pores, bubbles, or cracks, being not possible to verify microstructural differences among the produced formulations (Fig. 4a). However, the freeze-dried swollen CGP/PVA films evidenced a different pattern of microstructure organization, probably related to the film composition. The concentration of oxidizing agent ($NaIO_4$) and polymers (CGP and PVA) affected the microstructural morphology of the swollen films, with a group containing a varied content of interconnected pores with different sizes and morphologies

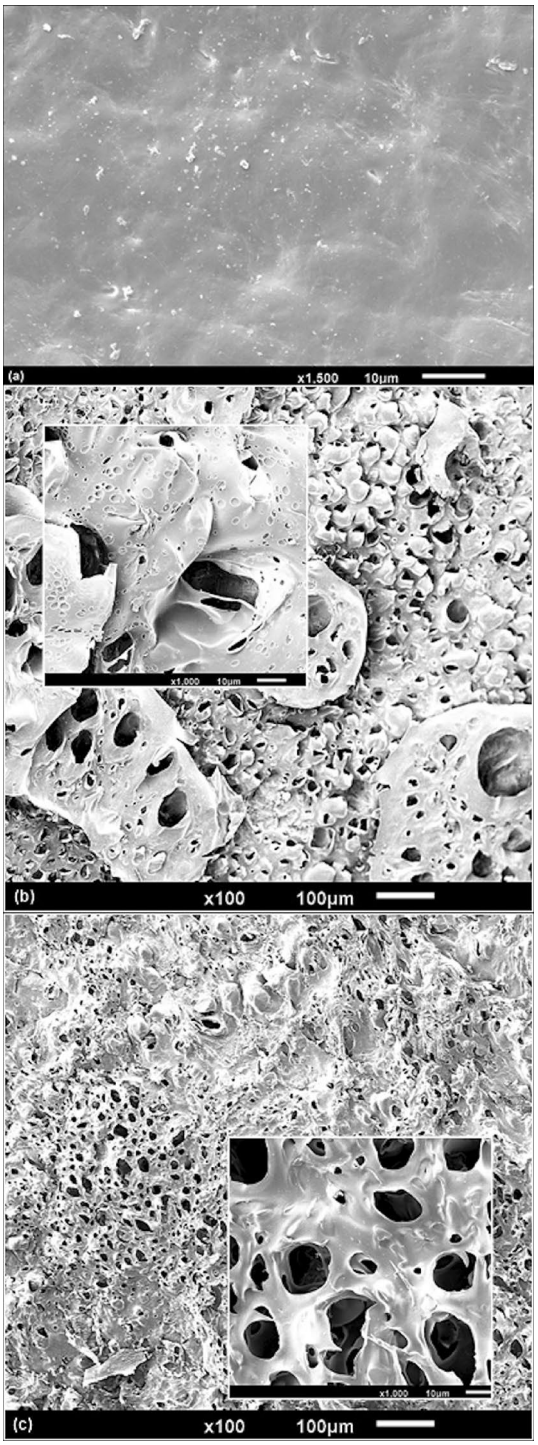

Fig. 4 Scanning electron micrographs of CGP/PVA films: **a** typical microstructure of a non-swollen CGP/PVA film; **b** surface microstructure of CGP/PVA film from formulation F1 (1% CGP; 3% PVA; and 0.5 mol L^{-1} $NaIO_4$) after swelling and lyophilization; and **c** surface microstructure of CGP/PVA film from formulation F8 (2% CGP; 6% PVA; and 0.5 mol L^{-1} $NaIO_4$) after swelling and lyophilization. Inserts were added to the micrographs (**b**, **c**) to provide a better understanding of the structural changes caused by the swelling process

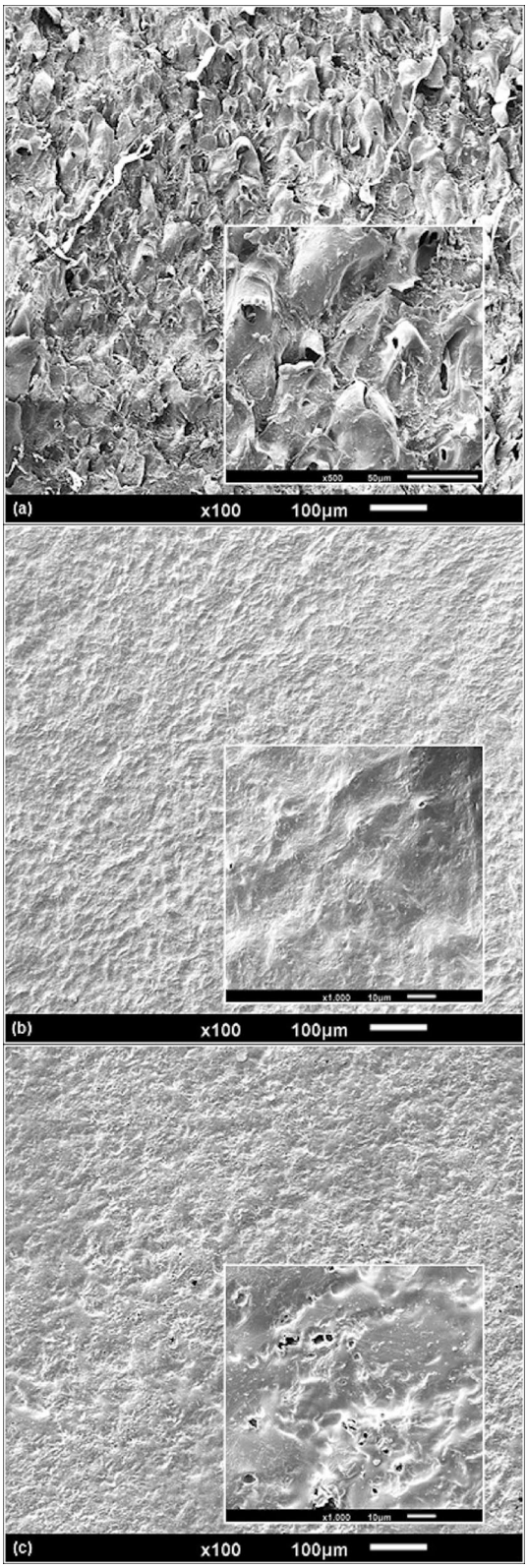

Fig. 5 Scanning electron micrographs showing the surface microstructure of swollen CGP/PVA films: **a** formulation F3 (3% CGP; 3% PVA; and 0.75 mol L^{-1} $NaIO_4$); **b** formulation F4 (1% CGP; 4.5% PVA; and 1.0 mol L^{-1} $NaIO_4$); and **c** formulation F7 (1% CGP; 6% PVA; and 0.75 mol L^{-1} $NaIO_4$). Inserts were added to the micrographs to understand better the structural changes caused by the swelling process

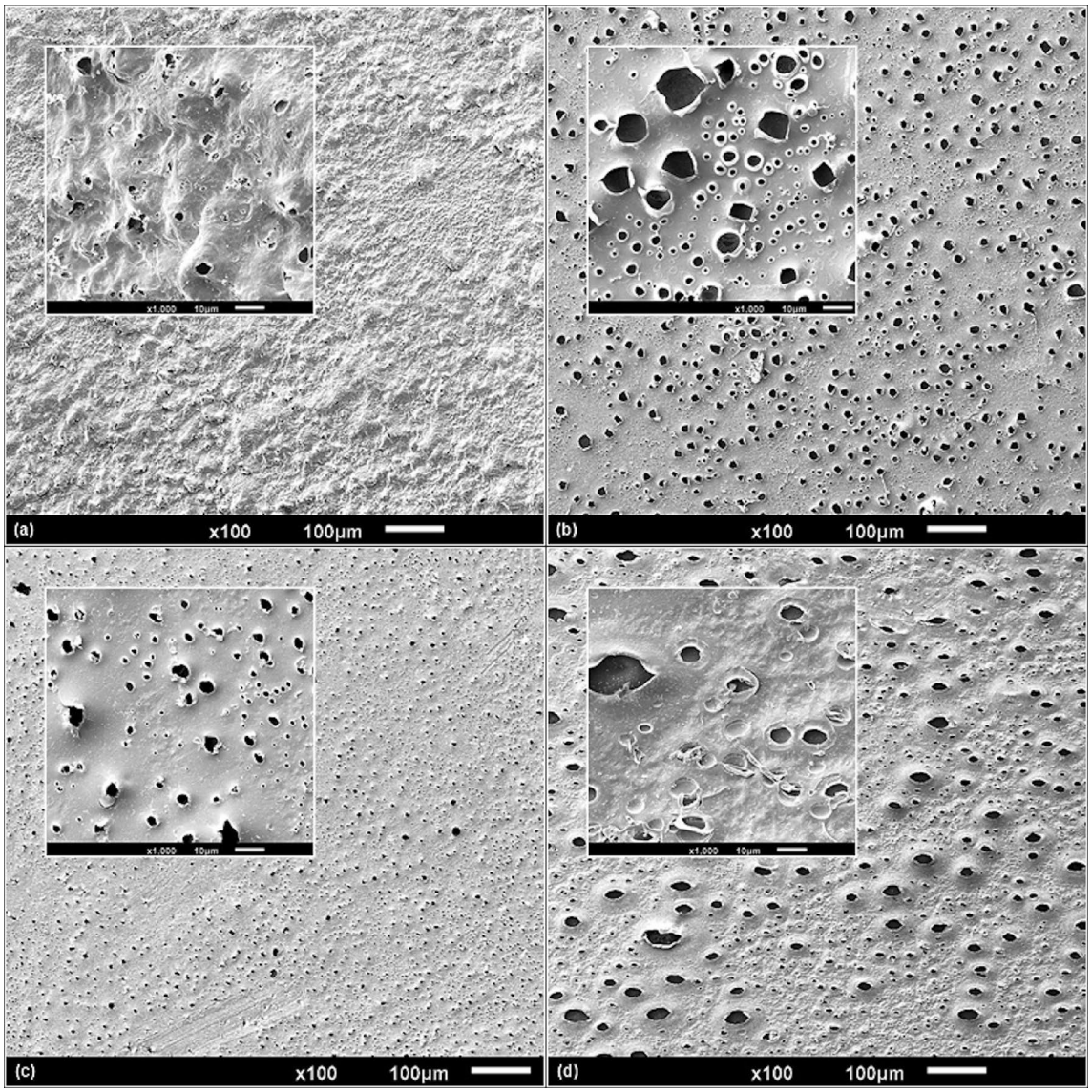

Fig. 6 Scanning electron micrographs showing the surface microstructure of swollen CGP/PVA films: **a** formulation F2 (2% CGP; 3% PVA; and 1.0 mol L^{-1} $NaIO_4$); **b** Formulation F5 (2% CGP; 4.5% PVA; and 0.75 mol L^{-1} $NaIO_4$); **c** formulation F6 (3% CGP; 4.5% PVA; and 0.5 mol L^{-1} $NaIO_4$); and **d** formulation F9 (3% CGP; 6% PVA; and 1.0 mol L^{-1} $NaIO_4$). Inserts were added to the micrographs to understand better the structural changes caused by the swelling process

(Fig. 4b, c) and another group without defined pores (Figs. 5 and 6).

Although the concentrations of CGP and PVA play an important role in network formation, $NaIO_4$ concentration is a key factor determining the extension of three-dimensional changes in the swollen films. For the CGP/PVA films from formulations F1 and F8, produced with the lowest concentration of $NaIO_4$ (0.5 mol L^{-1}), a porous tridimensional structure was observed due to the freeze-drying process. In this case, the absorbed water has acted as a porogen. During the freezing process, the ice crystals formed in the CGP/PVA network caused an expansion in the film's three-dimensional structure, with a physical separation of the polymer chain entanglements and their concentration at the interface of the ice crystals. Then, the ice crystals were sublimated during lyophilization, forming a porous structure of interconnected polymer chains (de Lacerda Bukzem et al. 2021).

Despite these two formulations presenting microporosity, it is evident that the polymers' content influenced the shape and size of the pores. SEM images showed an irregular incidence of porous structures in the CGP/PVA film from formulation F1, apparently due to a rupture of structures like vesicles in the film surface. Considering the highly branched characteristic of CGP, the oxidation effect of NaIO4 on the vicinal hydroxyls (C2 and C3) on CGP may be mild, and consequently, there is a lower number of interaction points

available to react with PVA (Cruz et al. 2019b). In this case, the resultant three-dimensional structure of CGP/PVA from formulation F1 has regions more cohesive and resistant to extension, corresponding to the interaction points between CGP and PVA and other more flexible areas referred to the polymer chain entanglements from CGP. These differences in the film network organization can explain the vesicle-like structures observed in film formulation F1 (Fig. 4b), in which the regions containing CGP weakly crosslinked with PVA will be more flexible and extensible than the regions showing a large number of interconnections between CGP and PVA.

On the other hand, for the formulation F2, the increase in the content of each polymer contributed to organizing the films in a more homogeneous network, reflecting in a three-dimensional system with increased microporosity (Fig. 4c). The porous structure of these two formulations of CGP/PVA films can provide an interesting matrix for drug absorption and release, as well as for cell growth (Nissi et al. 2023; Enache et al. 2022). Generally, the number and size of pores in a support can affect the number of molecules entrapped in the film network (Bi et al. 2016). In this case, the differences in pore incidence and morphology in the CGP/PVA films might increase the diversity of biomolecules to be entrapped into these matrices. In addition, polymer-based porous films are reported to be excellent materials for wound dressing applications since they can maintain the moist surface of the wound, facilitate gas exchange, and remove excess exudates, which favors tissue regeneration (Kaolaor et al. 2019; Shitole et al. 2019; Agarwal et al. 2022).

The SEM micrographs for the other CGP/PVA films have shown different surface microstructures without defined pores. For film formulation F3, a vesicle-like structure was also observed (Fig. 5a). However, there is no evidence of pore formation. Similar to that was observed for CGP/PVA formulation F1, it is possible that the content of oxidizing agent ($NaIO_4$) used was insufficient to create reactive sites in CGP and PVA to produce a homogeneous network, and considering the branched structure of CGP, the non-linked regions could present higher expansion during the formation of the ice crystal, forming the spongy-form surface structure observed in Fig. 5a.

For the CGP/PVA films from formulations F4 (Fig. 5b) and F7 (Fig. 5c), it was observed a homogeneous and cohesive microstructure with slight differences compared to the unswollen film (Fig. 4a). This result can be explained due to the high concentration of $NaIO_4$ and PVA in these formulations, which leads to a higher extent of oxidation and an increase in the number of cross-linkages between GCP and PVA, resulting in a more compact matrix that did not expand during the formation of ice crystals.

For the other film formulations (F2, F5, F6, and F9), it was observed the presence of some cracks and disrupted bubbles, but without defined pores (Fig. 6). It is possible that during swelling, some regions in which the polymers were weakly connected had a more prominent water absorption and during freezing, the expansion of ice crystals caused a rupture of the formed bubbles.

Despite the absence of pores, these CGP/PVA films remain attractive as wound-healing plasters due to their potent properties of swelling. However, the lack of pores is a disadvantage for the use of these films as plasters for extended periods (Shalaby et al. 2022) because they can restrict oxygen diffusion and do not effectively control water loss, making necessary a frequent replacement of the plaster to avoid delay in the wound healing. Nevertheless, considering that CGP/PVA films were previously characterized as non-irritative skin materials (Chagas et al. 2022), this limitation of use is not a drawback that highly interferes with the potential of using these materials for wound healing applications. Additionally, considering the possibility of these films acting as controlled drug delivery systems, they can be used as medicated plaster for pain relief in non-injured skin.

Entrapment efficiency of the NSAIDs onto the CGP/PVA films

The feasibility of functionalizing the CGP/PVA films with NSAIDs was tested, and the entrapment efficiency results of ketoprofen and diclofenac sodium are shown in Table 5. The entrapment efficiency of diclofenac sodium in the different CGP/PVA formulations ranged from 0 to 75.6%, while for ketoprofen entrapment these values varied from 0% to 32.2%.

Results from the multivariate analysis showed that the composition of the CGP/PVA films affected each NSAID's entrapment (Table 3). The evaluation of the relationship between the film components and the entrapment efficiency

Table 5 Results of entrapment efficiency (%EE) for diclofenac sodium and ketoprofen onto the CGP/PVA films produced as established by the fractional 3^{3-1} factorial design

Formulation	Entrapment efficiency (%EE)[a]	
	Diclofenac sodium	Ketoprofen
F1	50.3 ± 0.01	0.2 ± 0.06
F2	75.6 ± 0.12	9.9 ± 0.07
F3	17.1 ± 0.21	24.6 ± 0.24
F4	60.7 ± 0.05	17.8 ± 0.19
F5	0.0	31.3 ± 0.74
F6	18.6 ± 0.06	22.5 ± 0.15
F7	8.0 ± 0.71	0.0
F8	8.0 ± 0.84	32.2 ± 0.14
F9	48.4 ± 0.16	30.9 ± 0.06

[a]The values are presented as means and standard deviations ($n = 4$)

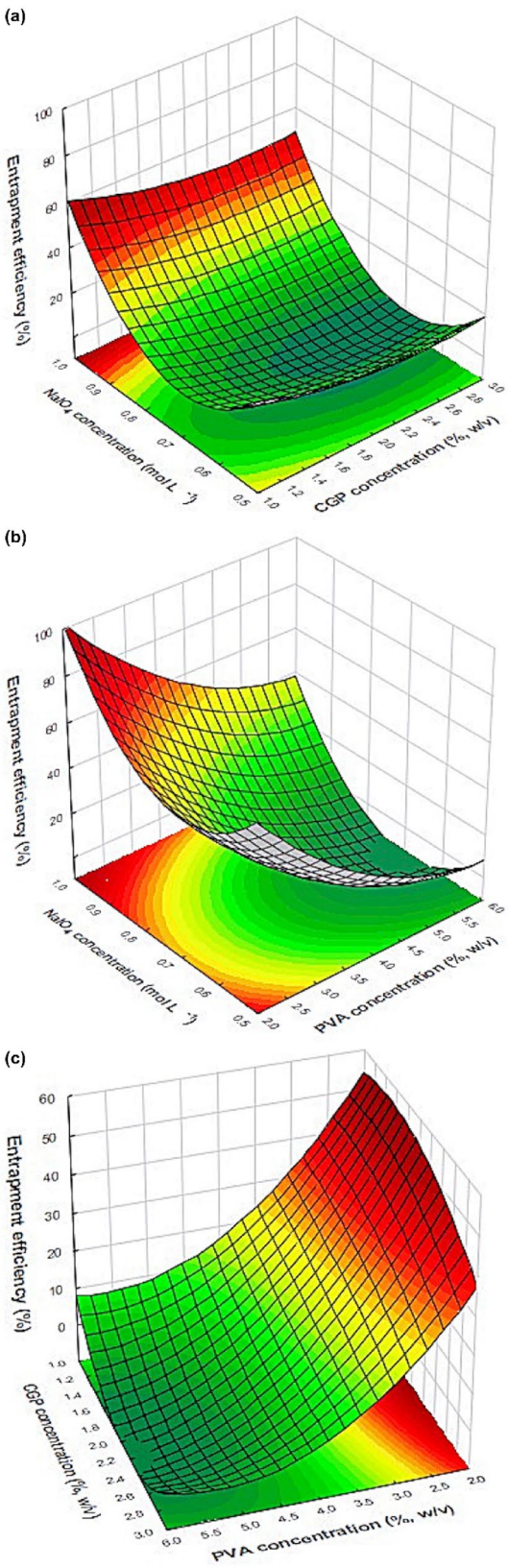

Fig. 7 Response surface plot obtained in the 3^{3-1} fractional factorial design for the entrapment efficiency of diclofenac sodium in the CGP/PVA films as a function of the variables significantly affecting the response ($p < 0.05$). **a** Three-dimensional plot showing the effect of oxidizing agent ($NaIO_4$) and CGP content on the diclofenac entrapment efficiency. This plot was drawn by setting the PVA concentration at 4.5% (*w*/*v*). **b** Three-dimensional plot showing the effect of PVA and CGP content on the drug entrapment efficiency. This plot was drawn by setting the $NaIO_4$ concentration at 0.75 mol $L.^{-1}$. **c** Three-dimensional plot showing the effect of oxidizing agent ($NaIO_4$) and PVA content on the response. The plot was drawn by setting the GPC concentration at 2.0% (*w*/*v*)

shows that the most pronounced effect was observed for the quadratic term of oxidizing agent concentration, negatively affecting the response. In addition, CPG and PVA concentrations and interaction between the quadratic term of CGP and the linear term of PVA also negatively affected the drug entrapment efficiency (Table 3). These overall negative effects on the entrapment efficiency of diclofenac may be a result of the film network organization since large increases in the content of $NaIO_4$ lead to increases in the number of cross-linkages between CGP and PVA (Fig. 7a, b), resulting in a more compact matrix with lower ability of drug loading. Furthermore, the drug entrapment efficiency strongly depends on the drug solubility in the film matrix, which is related to the composition of polymers and drug–polymers interaction (Silva et al. 2021). Considering the negative charge of diclofenac sodium, increases in CGP concentration will increase the overall negative charge of the produced film, and therefore, the charge repulsion between the drug and the polymer will result in a reduction in the entrapment of diclofenac into the inner part of the produced film (Fig. 7a, c). On the other hand, the simultaneous linear increase in the content of CGP and PVA leads to a general increase in the cross-linkage points, reducing the overall negative charge of the produced film and therefore diminishing the drug–polymer charge repulsion and favoring the drug entrapment into the film matrix (Fig. 7c).

The data from entrapment efficiency (EE) were fitted to the second-order polynomial model, and the correlations between the response and the variables were expressed by the following equation:

$$\begin{aligned} \mathrm{EE}_{\mathrm{diclofenac}}(\%) = {} & 332.46 + 64.37X_1 - 18.73X_1^2 \\ & - 25.02X_2 + 3.61X_2^2 - 747.39X_3 \\ & + 538.85X_3^2 - 20.91X_1X_2 \\ & + 5.49X_1^2X_2 \left(r^2 = 0.99\right), \end{aligned} \tag{9}$$

where X_1 denotes de concentration of CGP (%, *w*/*v*), X_2 denotes de concentration of PVA (% *w*/*v*), and X_3 denotes the concentration of oxidizing agent (mol L^{-1}). The high proportions of variability ($r^2 = 0.999$) in the response model can be explained successfully by the experimental model.

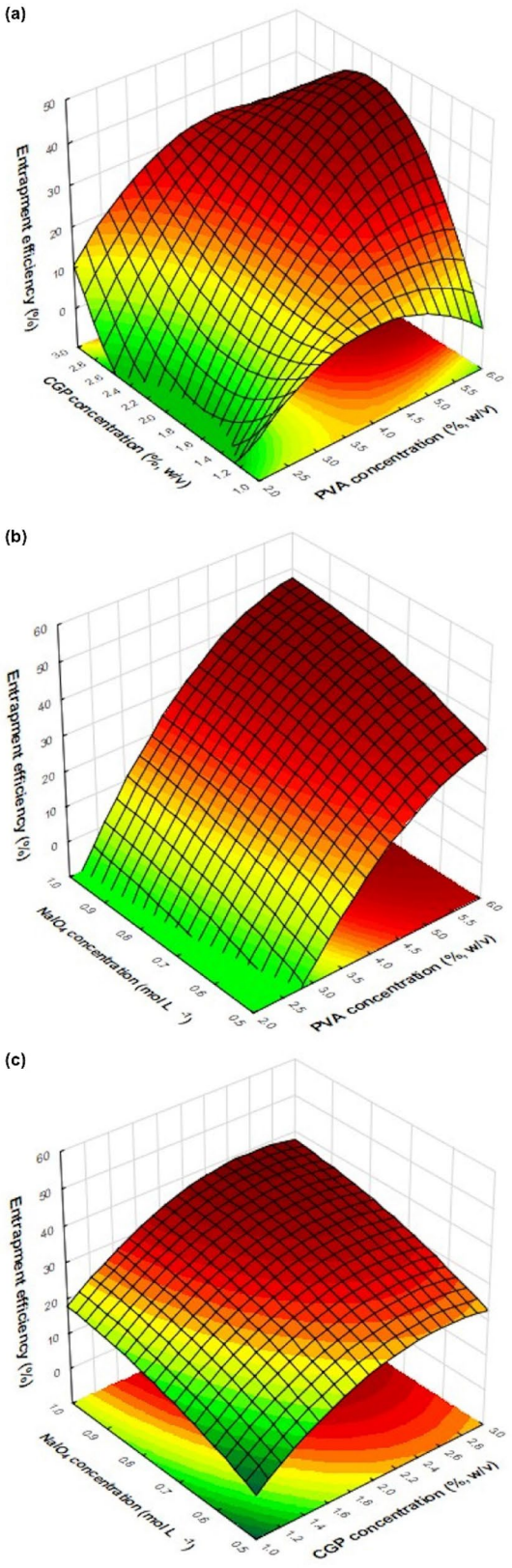

Fig. 8 Response surface plot obtained in the 3^{3-1} fractional factorial design for the entrapment efficiency of ketoprofen in the CGP/PVA films as a function of the variables that significantly affected the response ($p < 0.05$). **a** Three-dimensional plot showing the effect of PVA and CGP content on the drug entrapment efficiency. This plot was drawn by setting the $NaIO_4$ concentration at 0.75 mol $L.^{-1}$. **b** Three-dimensional plot showing the effect of oxidizing agent ($NaIO_4$) and PVA content on the response. The plot was drawn by setting the GPC concentration at 2.0% (*w/v*). **c** Three-dimensional plot showing the effect of oxidizing agent ($NaIO_4$) and CGP content on the diclofenac entrapment efficiency. This plot was drawn by setting the PVA concentration at 4.5% (*w/v*)

However, a large value of r^2 is not enough to always assure that the regression model is good since increases in the number of variables will increase de the r^2 value independent if these variables are statically significant. For this reason, it is better to evaluate the model's adequacy using the adjusted r^2 value, which is a measure that indicates the fitness of the model, and it should be over 90%. Considering that r^2 and adj-r^2 values for the model are very close, it is possible to guarantee that the insignificant terms have not been included in the model. In addition, the adj-r^2 value indicated that 99.99% of the experimental data from entrapment efficiency of diclofenac were in agreement with the predicted values, assuring that the experimental model can successfully explain this response.

Considering the data from ketoprofen entrapment, multivariate analysis ($r^2 = 0.99$) showed that all variables positively influenced the response (Table 3). Considering the hydrophobic nature of ketoprofen, the higher the content of polymers, the higher the hydrophobic spots in the film matrix (Fig. 2), increasing the amount of ketoprofen able to penetrate deeply into the polymeric matrix (Fig. 8a).

The regression analysis showed a good fit of experimental values to the second-order polynomial model as a function of significant factors. The mathematical model is represented in the following equation:

$$\begin{aligned} EE_{ketoprofen}(\%) = {} & 76.83 - 218.23X_1 + 54.83X_1^2 \\ & - 17.42X_2 - 3.36X_2^2 + 95.00X_3 \\ & - 42.93X_3^2 + 58.24X_1X_2 \\ & - 14.07X_1^2X_2 \ \left(r^2 = 0.99\right) \end{aligned} \quad (10)$$

where X_1 denotes de concentration of CGP (%, *w/v*), X_2 denotes de concentration of PVA (% w/v), and X_3 denotes the concentration of oxidizing agent (mol L^{-1}). The high adj-r^2 value (0.99) confirmed the model's adequacy, which indicates that 99.99% of the experimental data agreed with the predicted values.

The correlation between the independent variables on ketoprofen's entrapment efficiency was investigated using response surface methodology. Despite the lower entrapment efficiency for ketoprofen compared to diclofenac,

Fig. 8 shows a well-defined region of maximum values for ketoprofen entrapment onto CGP/PVA films. As can be seen, higher percentages of entrapment were found in the CGP/PVA films containing at least 4.5% of PVA and 2% of CGP in their formulation. Based on these results, formulation F8 (32.2% entrapment) was chosen to evaluate the ketoprofen release profile.

It is important to point out that the differences in the magnitude of entrapment as well as the behavior of drug retention on the CGP/PVA films can also be ascribed to the intrinsic characteristics of each drug that will dictate the intermolecular interactions with the polymeric matrix (Fig. 2). The aromatic rings present in both ketoprofen and diclofenac will probably interact with the CGP/PVA structure through weak intermolecular bonding forces (i.e., hydrophobic interactions and Van der Waals force) (Silva et al. 2021; Freitas et al. 2018). Considering the weakness of these interactions, it is possible to infer that initially the diffusion forces stimulate the migration of the drugs from the solution to the swollen structure of the CGP/PVA films. However, a prolonged reaction time can lead to a lixiviation of the entrapped drug back to the solution. This effect can explain the differences in the magnitude of entrapment for ketoprofen and diclofenac. Probably the interaction forces between the functional groups of ketoprofen and the CGP/PVA structure were weaker than those between diclofenac and CGP/PVA films leading to higher values of entrapment efficiency for diclofenac (Fig. 2).

In vitro drug release

The in vitro drug release of diclofenac sodium and ketoprofen from CGP/PVA films in sodium phosphate buffer at pH 7.4 was investigated and their kinetics are shown in Fig. 9.

As can be seen, the drugs were released from CGP/PVA films in a controlled manner with a burst effect within the first hour followed by a slow and continuous release for the next 6 h. This initial burst effect can be attributed to the release of weakly bonded drug molecules (Lai et al. 2018; Feng et al. 2020). On the other hand, the sustained release of the drugs is likely related to the formation of host–guest complexes between polymers and drug molecules (Oroujeni et al. 2018). The formation of host–guest complexes can contribute to enhancing the intermolecular association between the CGP/PVA matrix and drug molecules leading to a delay in the release of both, ketoprofen and diclofenac (Fig. 2). Considering the application of the CGP/PVA films as wound-care dressing materials, it is possible that the wound exudate or blood would increase the rate of drug release due to the improvement of swelling of the film matrix or even because of the concentration gradient that favor the release of the drug from the inner sites in the CGP/PVA films to the interstitial space of the injured tissue.

It is interesting to point out that the speed of ketoprofen release was lower than that observed for diclofenac sodium. These differences in the release profile can be due to the intrinsic characteristics of the CGP/PVA films as well as the hydrophilicity/hydrophobicity of the drugs (Fig. 2). In the first hour the release profile may be dictated by the swelling of CGP/PVA films, since the water molecules will enter the film's network and stimulate the drug's diffusion out. In

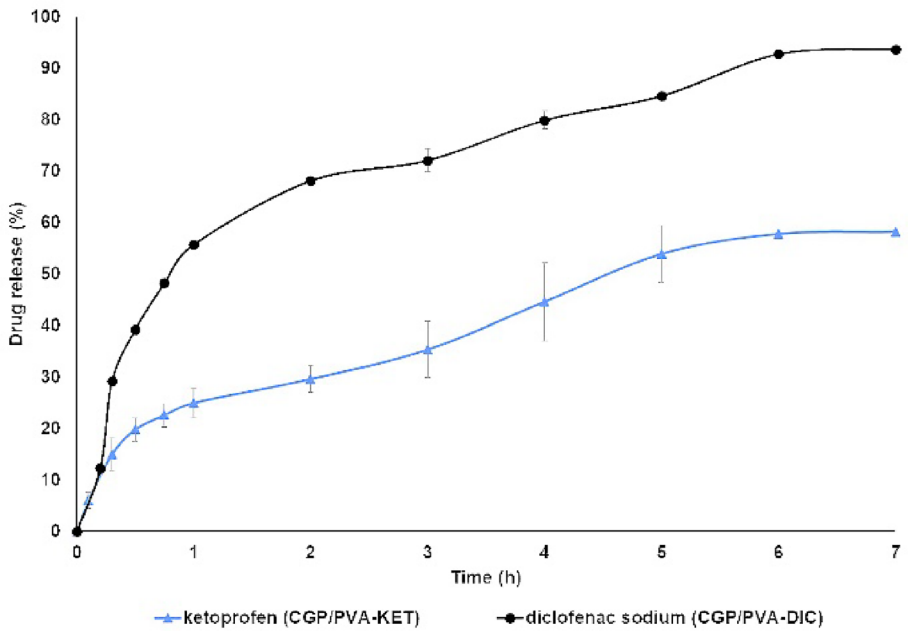

Fig. 9 In vitro release profile of ketoprofen and diclofenac sodium from the CGP/PVA films. Results were presented as percentages of cumulative release over time, and the vertical bars correspond to the standard deviation of the data

Table 6 Results for the model fitting of the release profiles for ketoprofen (CGP/PVA–KET) and diclofenac sodium (CGP/PVA–DIC)

Formulation	Kinetic models			
	Zero-order	First order	Higuchi	Korsmeyer–Peppas
CGP/PVA–KET	0.9545	0.8409	0.9389	**0.9985**
CGP/PVA–DIC	0.8980	0.9173	0.9928	**0.9937**

Bold values indicate $p = 0.05$

this case, despite the lower swelling capacity of the CGP/PVA film formulation F2 when compared to formulation F8 (Fig. 1), the more hydrophilic feature of diclofenac sodium associated with a higher amount of entrapped drug may explain the higher percentage of drug released.

After the equilibrium of swelling, the drug release can be correlated to the intrinsic characteristics of each drug. The hydrophilic nature of diclofenac sodium allows for better drug diffusion from CGP/PVA to the phosphate solution, with maximum release values around 94% (~7.1 mg). On the other hand, despite the similar release profile, the magnitude of ketoprofen release was lower than those observed for diclofenac, with a release of around 60% (~1.9 mg) being achieved. In this case, the hydrophobic nature of ketoprofen negatively interfered with the diffusion process. As reported by Liu et al. (Liu et al. 2016), during the release process, hydrophilic drug aggregates migrate from the polymer network and enter into water, and disperse in a unimolecular form quickly, facilitating their dissolution. However, hydrophobic drugs can cluster together, forming aggregates that retard the diffusion process and will not disperse and dissolve quickly after migration from the polymer network, which will retard their dissolution.

Furthermore, it can be seen that the drug release took about 7 h to reach its maximum for both entrapped drugs (Fig. 9), suggesting that CGP/PVA–KET and CGP/PVA–DIC could be tested as multifunctional wound-care dressings presenting a prolonged release of anti-inflammatory drugs. The slow release of diclofenac and ketoprofen from the CGP/PVA films may prolong their analgesic and anti-inflammatory activities, avoiding toxic side effects, preventing sub-therapeutic levels of the drugs, and reducing the frequency of the need for subsequent dressing changes.

Analysis of kinetic models

Evaluating drug release by an appropriate mathematical model can support interpreting and comprehending the mechanisms controlling the release process (Tan et al. 2019; Bataglioli et al. 2019). Different models were fitted to the experimental data to determine the mechanism governing drug release from the films. The best model was selected according to the regression coefficient (r^2) determined from the linear regression fit for each model (Table 6).

Results from regression analysis evidenced that the in vitro drug release of CGP/PVA–KET and CGP/PVA–DIC has shown a good fit with the Korsmeyer–Peppas model (Table 6), indicating that drug release follows a diffusion mechanism. However, the values of the release exponent indicated a different release behavior between the films. For CGP/PVA–KET films, the value of the release exponent ($n = 0.42$) suggests that the Fickian diffusion is the dominant mechanism of ketoprofen release (Ritger and Peppas 1987; Kashani et al. 2021). The release exponent (n) of the Korsmeyer–Peppas equation for CGP/PVA–DIC was found to be 0.51, indicating that the release occurred according to a non-Fickian transport, in which this process is driven by both relaxation of the CGP/PVA matrix and diffusion of the drug (Ritger and Peppas 1987; Bataglioli et al. 2019; Kashani et al. 2021).

Conclusions

In this study, the characteristics of wound-care dressing films prepared by blending polyvinyl alcohol and cashew gum polysaccharide were evaluated. Using a 3^{3-1} fractional factorial design it was possible to distinguish the effect of each component on the physicochemical and morphological properties of the produced materials and to determine the best formulation for the entrapment of NSAIDs. CGP/PVA films produced using 2% CGP, 3% PVA and 1 mol L^{-1} $NaIO_4$ showed the best performance of entrapment for diclofenac sodium (75.6%), with the drug release profile following a non-Fickian transport. Regarding ketoprofen entrapment (32.2%), the best formulation was achieved by blending 2% CGP, and 6% PVA with 0.5 mol L^{-1} of $NaIO_4$, with a drug release following a Fickian diffusion mechanism. In addition, drugs were released in a controlled manner with a sustained in vitro release over 7 h being observed. Regarding the application of these CGP/PVA films for use as wound-care dressings, their high swelling capacity would allow the removal of excess exudates and the maintenance of a local moist environment. Moreover, the sustained release of ketoprofen and diclofenac would prolong the drug's action time, improving therapeutic efficacy and reducing the frequency of wound dressing changes. Despite the absence of pores in some film formulations, which will demand a more frequent replacement of the plaster, the skin non-irritative property of these films constitutes an advantage that could overcome this drawback. In addition, considering the controlled released profile of the produced CGP/PVA films, it is also possible to suggest their use as medicated plasters for pain management.

However, further in vitro and in vivo tests should be performed to confirm the potentialities of CGP/PVA films as membranes for clinical use. Additional studies have also to be conducted to determine the long-term storage stability of the CGP/PVA films and the best storage conditions.

Acknowledgements This work was supported by the National Council on Scientific and Technological Development / Conselho Nacional de Desenvolvimento Científico e Tecnológico – CNPq – Brazil [Grant number 402468/2013-9] and Coordination for the Improvement of Higher Education Personnel / Coordenação de Aperfeiçoamento de Pessoal de Nível Superior – CAPES – Brazil [Finance Code 001]. Maurício V. Cruz and Kátia F. Fernandes also thank FAPEG and CNPq for the fellowship support.

Author contributions CNSS and MVC participated in the conceptualization, formal analysis, investigation, methodology determination, experimental validation, and writing of the original draft. Kátia F Fernandes participated in the conceptualization, formal analysis, methodology determination, supervision, data visualization, founding acquisition, and writing of the original draft. KAB participated in the conceptualization, formal analysis, investigation, methodology determination, data analysis and visualization, funding acquisition, project administration, supervision, writing of the original draft, and editing/revision of the final version of the manuscript.

Data availability The data presented in this study are available on request from the corresponding author.

Declarations

Conflict of interest The authors declare that they have no conflict of interest in the publication.

References

Abdel-Mageed HM, Abd El Aziz AE, Abdel Raouf BM, Mohamed SA, Nada D (2022) Antioxidant-biocompatible and stable catalase-based gelatin–alginate hydrogel scaffold with thermal wound healing capability: immobilization and delivery approach. 3 Biotech 12(3):73. https://doi.org/10.1007/s13205-022-03131-4

Agarwal A, Rao GK, Majumder S, Shandilya M, Rawat V, Purwar R, Verma M, Srivastava CM (2022) Natural protein-based electrospun nanofibers for advanced healthcare applications: progress and challenges. 3 Biotech 12(4):92. https://doi.org/10.1007/s13205-022-03152-z

Al-Lawati H, Vakili MR, Lavasanifar A, Ahmed S, Jamali F (2019) Delivery and biodistribution of traceable polymeric micellar diclofenac in the rat. J Pharm Sci 108(8):2698–2707. https://doi.org/10.1016/j.xphs.2019.03.016

Bataglioli RA, Taketa TB, Neto JBMR, Lopes LM, Costa CAR, Beppu MM (2019) Analysis of pH and salt concentration on structural and model-drug delivery properties of polysaccharide-based multilayered films. Thin Solid Films 685:312–320. https://doi.org/10.1016/j.tsf.2019.06.039

Bi C, Jackson A, Vargas-Badilla J, Li R, Rada G, Anguizola J, Pfaunmiller E, Hage DS (2016) Entrapment of alpha1-acid glycoprotein in high-performance affinity columns for drug-protein binding studies. J Chromatogr B 1021:188–196

Chagas AdLd, Oliveira LPd, Cruz MV, Melo RMd, Miguel MP, Fernandes KF, Menezes LBd (2022) Polysaccharide-based membrane biocompatibility study of *Anacardium occidentale* L. and polyvinyl alcohol after subcutaneous implant in rats. Materials 15(4):1296

Chandika P, Kim MS, Khan F, Kim YM, Heo SY, Oh GW, Kim NG, Jung WK (2021) Wound healing properties of triple cross-linked poly (vinyl alcohol)/methacrylate kappa-carrageenan/chitooligosaccharide hydrogel. Carbohydr Polym 269:118272. https://doi.org/10.1016/j.carbpol.2021.118272

Cruz MV, Jacobowski AC, Macedo MLR, Batista KA, Fernandes KF (2019a) Immobilization of antimicrobial trypsin inhibitors onto cashew gum polysaccharide/PVA films. Int J Biol Macromol 127:433–439

Cruz MV, Pereira-Júnior MA, Batista KA, Fernandes KF (2019b) Use of statistical design strategies to produce biodegradable and eco-friendly films from cashew gum polysaccharide and polyvinyl alcohol. Materials 12(7):1149

de Lacerda Bukzem A, dos Santos DM, Leite IS, Inada NM, Campana-Filho SP (2021) Tuning the properties of carboxymethylchitosan-based porous membranes for potential application as wound dressing. Int J Biol Macromol 166:459–470. https://doi.org/10.1016/j.ijbiomac.2020.10.204

Enache A-C, Samoila P, Cojocaru C, Bele A, Bostanaru A-C, Mares M, Harabagiu V (2022) Amphiphilic chitosan porous membranes as potential therapeutic systems with analgesic effect for burn care. Membranes 12(10):973

Feng W, Feng C, Wang B, Jing A, Li G, Xia X, Liang G (2020) An amorphous calcium phosphate for drug delivery: ATP provides a phosphorus source and microwave-assisted hydrothermal synthesis. Mater Today Commun 25:101455. https://doi.org/10.1016/j.mtcomm.2020.101455

Feng P, Luo Y, Ke C, Qiu H, Wang W, Zhu Y, Hou R, Xu L, Wu S (2021) Chitosan-based functional materials for skin wound repair: mechanisms and applications. Front Bioeng Biotechnol 9:650598. https://doi.org/10.3389/fbioe.2021.650598

Freitas ED, Rosa PCP, Silva MGC, Vieira MGA (2018) Development of sericin/alginate beads of ketoprofen using experimental design: formulation and in vitro dissolution evaluation. Powder Technol 335:315–326

Gudin J, Nalamachu S (2020) Utility of lidocaine as a topical analgesic and improvements in patch delivery systems. Postgrad Med 132(1):28–36. https://doi.org/10.1080/00325481.2019.1702296

Kaolaor A, Phunpee S, Ruktanonchai UR, Suwantong O (2019) Effects of β-cyclodextrin complexation of curcumin and quaternization of chitosan on the properties of the blend films for use as wound dressings. J Polym Res 26(2):43. https://doi.org/10.1007/s10965-019-1703-y

Kashani HM, Madrakian T, Afkhami A (2021) Development of modified polymer dot as stimuli-sensitive and 67Ga radio-carrier, for investigation of in vitro drug delivery, in vivo imaging and drug release kinetic. J Pharm Biomed Anal 203:114217. https://doi.org/10.1016/j.jpba.2021.114217

Katiyar S, Singh D, Kumari S, Srivastava P, Mishra A (2022) Novel strategies for designing regenerative skin products for accelerated wound healing. 3 Biotech 12(11):316. https://doi.org/10.1007/s13205-022-03331-y

Khan YS, Gutiérrez-de-Terán H, Åqvist J (2018) Molecular mechanisms in the selectivity of nonsteroidal anti-inflammatory drugs. Biochemistry 57(7):1236–1248. https://doi.org/10.1021/acs.biochem.7b01019

Lai Y-L, Cheng P-Y, Yang C-C, Yen S-K (2018) Electrolytic deposition of hydroxyapatite/calcium phosphate-heparin/gelatin-heparin tri-layer composites on NiTi alloy to enhance drug loading and prolong releasing for biomedical applications. Thin Solid Films 649:192–201. https://doi.org/10.1016/j.tsf.2018.01.051

Lima MR, Paula HCB, Abreu FOMS, Silva RBC, Sombra FM, Paula RCM (2018) Hydrophobization of cashew gum by acetylation

mechanism and amphotecirin B encapsulation. Int J Biol Macromol 108:523–530
Liu L, Bai S, Yang H, Li S, Quan J, Zhu L, Nie H (2016) Controlled release from thermo-sensitive PNVCL-co-MAA electrospun nanofibers: the effects of hydrophilicity/hydrophobicity of a drug. MaterSci Eng C 67:581–589
Mendyk A, Jachowicz R (2007) Unified methodology of neural analysis in decision support systems built for pharmaceutical technology. Expert Syst Appl 32:1124–1131
Moreira BR, Batista KA, Castro EG, Lima EM, Fernandes KF (2015) A bioactive film based on cashew gum polysaccharide for wound dressing applications. Carbohyd Polym 122:69–76
Moreira BR, Pereira-Júnior MA, Fernandes KF, Batista KA (2020) An ecofriendly edible coating using cashew gum polysaccharide and polyvinyl alcohol. Food Biosci. https://doi.org/10.1016/j.fbio.2020.100722
Nissi JS, Vyaishnavi S, Sivaranjanee R, Sekar MP, Sundaramurthi D, Vadivel V (2023) Development and characterization of Morinda tinctoria incorporated electrospun PHBV fiber mat for wound healing application. Macromol Res 31(4):393–405. https://doi.org/10.1007/s13233-023-00149-2
Oroujeni M, Kaboudin B, Xia W, Jönsson P, Ossipov DA (2018) Conjugation of cyclodextrin to magnetic Fe3O4 nanoparticles via polydopamine coating for drug delivery. Prog Org Coat 144:154–161
Paranhos SB, Ferreira EdS, Canelas CAdA, da Paz SPA, Passos MF, da Costa CEF, da Silva ACR, Monteiro SN, Candido VS (2022) Chitosan membrane containing copaiba oil (*Copaifera* spp.) for skin wound treatment. Polymers 14(1):35
Piacentini E, Bazzarelli F, Poerio T, Albisa A, Irusta S, Mendoza G, Sebastian V, Giorno L (2020) Encapsulation of water-soluble drugs in Poly (vinyl alcohol) (PVA)- microparticles via membrane emulsification: influence of process and formulation parameters on structural and functional properties. Mater Today Commun 24:100967. https://doi.org/10.1016/j.mtcomm.2020.100967
Ritger PL, Peppas NA (1987) A simple equation for description of solute release II. Fickian and anomalous release from swellable devices. J Control Release 5:37–42
Sabbagh F, Muhamad II, Nazari Z, Mobini P, Taraghdari SB (2018) From formulation of acrylamide-based hydrogels to their optimization for drug release using response surface methodology. Mater Sci Eng C 92:20–25
Schindelin J, Arganda-Carreras I, Frise E, Kaynig V, Longair M, Pietzsch T, Preibisch S, Rueden C, Saalfeld S, Schmid B, Tinevez J-Y, White DJ, Hartenstein V, Eliceiri K, Tomancak P, Cardona A (2012) Fiji: an open-source platform for biological-image analysis. Nat Methods 9(7):676–682. https://doi.org/10.1038/nmeth.2019
Shalaby MA, Anwar MM, Saeed H (2022) Nanomaterials for application in wound Healing: current state-of-the-art and future perspectives. J Polym Res 29(3):91. https://doi.org/10.1007/s10965-021-02870-x
Sharma A, Mittal A, Puri V, Kumar P, Singh I (2020) Curcumin-loaded, alginate–gelatin composite fibers for wound healing applications. 3 Biotech 10(11):464. https://doi.org/10.1007/s13205-020-02453-5
Shehata S, Serpell CJ, Biagini SCG (2020) Architecture-controlled release of ibuprofen from polymeric nanoparticles. Mater Today Commun 25:101562. https://doi.org/10.1016/j.mtcomm.2020.101562
Shitole AA, Raut PW, Khandwekar A, Sharma N, Baruah M (2019) Design and engineering of polyvinyl alcohol based biomimetic hydrogels for wound healing and repair. J Polym Res 26(8):201. https://doi.org/10.1007/s10965-019-1874-6
Silva FE, Batista KA, Di-Medeiros MC, Silva CN, Moreira BR, Fernandes KF (2016) A stimuli-responsive and bioactive film based on blended polyvinyl alcohol and cashew gum polysaccharide. Mater Sci Eng, C 58:927–934
Silva CNSd, Di-Medeiros MCB, Lião LM, Fernandes KF, Batista KdA (2021) Cashew gum polysaccharide nanoparticles grafted with polypropylene glycol as carriers for diclofenac sodium. Materials 14(9):2115
Tan KX, Danquah MK, Pan S, Yon LS (2019) Binding characterization of aptamer-drug layered microformulations and in vitro release assessment. J Pharm Sci 108(9):2934–2941. https://doi.org/10.1016/j.xphs.2019.03.037